

RESEARCH ARTICLE

Human brain arteriovenous malformations express lymphatic-associated genes

Lorelei D. Shoemaker¹, Laurel F. Fuentes¹, Shauna M. Santiago¹, Breanna M. Allen¹, Douglas J. Cook², Gary K. Steinberg¹ & Steven D. Chang¹¹Department of Neurosurgery, Stanford Neuromolecular Innovation Program, Stanford University, 300 Pasteur Drive, Stanford, California, 94305²Centre for Neuroscience Studies and the Department of Surgery, Queen's University, Kingston, Ontario, Canada**Correspondence**

Steven D. Chang, Department of Neurosurgery, School of Medicine, Stanford University, 300 Pasteur Drive, Stanford, CA 94305. Tel: (650) 736-1134; Fax: (650) 725-5032; E-mail: sdchang@stanford.edu

Funding Information

This work was supported in part by funding from Robert C. and Jeannette Powell (S. D. C.), Sylvia Tang and Alan Wong (S. D. C.), the Leslie Munzer Neurological Institute of Long Island (S. D. C.), William and the late Paula Zappettini (S. D. C.), the Stanford Moyamoya and Angiogenesis Research Fund (G. K. S.), and Stanford Undergraduate Advising and Research.

Received: 27 June 2014; Revised: 8 October 2014; Accepted: 13 October 2014

Annals of Clinical and Translational Neurology 2014; 1(12): 982–995

doi: 10.1002/acn3.142

Abstract

Objective: Brain arteriovenous malformations (AVMs) are devastating, hemorrhage-prone, cerebrovascular lesions characterized by well-defined feeding arteries, draining vein(s) and the absence of a capillary bed. The endothelial cells (ECs) that comprise AVMs exhibit a loss of arterial and venous specification. Given the role of the transcription factor COUP-TFII in vascular development, EC specification, and pathological angiogenesis, we examined human AVM tissue to determine if COUP-TFII may have a role in AVM disease biology. **Methods:** We examined 40 human brain AVMs by immunohistochemistry (IHC) and qRT-PCR for the expression of COUP-TFII as well as other genes involved in venous and lymphatic development, maintenance, and signaling. We also examined proliferation and EC tube formation with human umbilical ECs (HUVEC) following COUP-TFII overexpression. **Results:** We report that AVMs expressed COUP-TFII, SOX18, PROX1, NFATC1, FOXC2, TBX1, LYVE1, Podoplanin, and vascular endothelial growth factor (VEGF)-C, contained Ki67-positive cells and heterogeneously expressed genes involved in Hedgehog, Notch, Wnt, and VEGF signaling pathways. Overexpression of COUP-TFII alone in vitro resulted in increased EC proliferation and dilated tubes in an EC tube formation assay in HUVEC. **Interpretation:** This suggests AVM ECs are further losing their arterial/venous specificity and acquiring a partial lymphatic molecular phenotype. There was significant correlation of gene expression with presence of clinical edema and acute hemorrhage. While the precise role of these genes in the formation, stabilization, growth and risk of hemorrhage of AVMs remains unclear, these findings have potentially important implications for patient management and treatment choice, and opens new avenues for future work on AVM disease mechanisms.

Introduction

Brain arteriovenous malformations (AVMs) are vascular lesions characterized by the absence of a capillary bed and dilated vessels comprised of endothelial cells (ECs) with ambiguous venous and arterial identity. Diagnosis is commonly made following presentation of progressive neurological deficits, seizures, or hemorrhage. AVMs can occur anywhere in the brain and vary in size, blood flow volume, and venous drainage, all of which are factors that guide a challenging choice of treatment including monitoring, embolism, radiosurgery, and surgical resection.

There is evidence that AVMs are actively angiogenic and dynamic, express proliferation-associated proteins,^{1–3} and contain ECs that are highly proliferative, migrate more quickly and respond differently to various factors such as TGF- β in vitro, compared to control ECs.^{4–6} The disease is rare, with an incidence of <2 cases per 100,000 and a < 0.2% prevalence rate.⁷ No clear genetic link has yet been made, although several proteins have been implicated, including vascular endothelial growth factor (VEGF), angiopoietins, fibronectin, and matrix metalloproteinases.^{8,9} AVM research has been advanced by several animal models that exhibit vascular abnormalities,

but it is not clear if these completely recapitulate human disease.^{10–13} Many questions remain, including the underlying disease mechanism, the risk of hemorrhage and the most efficacious treatment plan.

The orphan steroid/thyroid hormone nuclear receptor COUP-TFII (also known as Apolipoprotein A-I regulatory protein 1 or NR2F2) has well described roles in angiogenesis, neural development, organogenesis, metabolism and disease.¹⁴ COUP-TFII serves as a key regulator in EC fate determination to establish both the venous system through inhibition of Notch signaling,^{15,16} and the lymphatic system through interactions with SOX18 and PROX1.^{17–19} In the adult, COUP-TFII is expressed at low levels in venous ECs and arterial smooth muscle cells but is largely absent in arterial ECs.¹⁶ Constitutive loss of COUP-TFII is lethal by embryonic day 10.5 (E10) in a murine model,²⁰ while an EC-specific loss of COUP-TFII is lethal at E12.¹⁶ Overexpression of COUP-TFII in ECs in transgenic mouse embryos results in malformations that resemble AVMs, with the loss of a capillary bed, fusion of arteries and veins, and arterial acquisition of venous-associated proteins.¹⁶ COUP-TFII also has a role in regulating cell proliferation and has been implicated in cancer, modulating both angiogenesis, and tumorigenesis via TGF- β signaling in human and mouse.^{15,21–23}

Given the key role of COUP-TFII in specifying venous and lymphatic fate and in pathological angiogenesis, we asked if COUP-TFII also plays a role in human brain AVMs. We report that AVMs expressed COUP-TFII and other lymphatic-associated genes, and that preoperative edema and acute hemorrhage were significantly correlated with the expression of a subset of these genes. Expression

analysis of selected genes involved in Hedgehog (HH), Notch, Wnt, and VEGF signaling pathways revealed heterogeneity in a subset of these AVMs. We also show that *in vitro* overexpression of COUP-TFII in human umbilical ECs (HUVECs) was sufficient to increase EC proliferation and tube dilation. These results suggest that human brain AVMs may be partially acquiring a lymphatic EC molecular signature. Given that the brain does not have a lymphatic system, these findings may have direct clinical relevance to the management and treatment of patients with brain AVMs and has highlighted future avenues for research.

Materials and Methods

Human AVM and control tissue

Tissue from 40 human brain AVM samples was obtained under consent during surgery in the Department of Neurosurgery at Stanford University with approval from Stanford's Institutional Review Board. AVM tissue was paraffin embedded for routine pathology. Depending on AVM size, additional portions were fresh frozen and stored at -80°C . A summary of patient demographics, AVM grade and treatment is outlined in Table 1. Normal human control brain (cortex) was obtained from the Stanford Cancer Center Tissue Bank.

Immunohistochemistry

Paraffin-embedded AVMs ($n = 29$) were sectioned into $4\ \mu\text{m}$ sections and deparaffinized. Appropriate antigen retrieval was performed for the following antibodies in

Table 1. Summary of AVM patient demographics and clinical history.

	IHC expression subjects ($n = 29$)		Gene profiling subjects ($n = 20$)	
	Female	Male	Female	Male
Number of patients	13	16	11	9
Median age at surgery \pm SD (y)	21 ± 11.9	36 ± 14.7	26 ± 13.2	41 ± 15.1
Self-reported Ethnicity (H/C/A/O)	5/3/2/3	6/1/2/7	3/3/3/2	3/2/1/3
Acute hemorrhage	3	11	6	4
Treatment modalities (S/ES/ERS)	9/4/0	2/13/1	2/8/1	5/3/1
Spetzler-Martin				
Grade 1	7	7	1	3
Grade 2	3	5	2	4
Grade 3	1	3	4	1
Grade 4	1	1	3	1
Grade 5	1	0	1	0

AVMs from 29 patients were analyzed by immunohistochemistry (IHC), from 20 patients by qRT-PCR and from nine patients by both techniques. Acute hemorrhage was defined as clinical presentation of hemorrhage immediately preceded by surgery. AVM, arteriovenous malformation; IHC, immunohistochemistry; H/C/A/O, Hispanic/Caucasian/Asian/Other; S/ES/ERS, Surgery (S)/Embolization and Surgery (ES)/Embolization, Radiosurgery and Surgery (ERS).

serial sections: COUP-TFII (mouse monoclonal, R&D Systems, Minneapolis, MN, 1:200), PROX1 (mouse monoclonal, Abcam, Cambridge, MA, 1:100), LYVE1 (rabbit polyclonal, Abcam, Cambridge, MA, 1:100), D2-40 (Podoplanin, mouse monoclonal, Dako, Carpinteria, CA, 1:100), CD31 (PECAM, rabbit monoclonal, Millipore, Temecula, CA, 1:300), Ki67 (rabbit polyclonal, Abcam, Cambridge, MA, 1:50). Sections were exposed to primary antibody at 4°C overnight and secondary antibody for 1 h, visualized with 3,3'-diaminobenzidine (DAB) and hematoxylin, and imaged using a Zeiss Axio Imager M2 microscope (Thornwood, NY).

Quantitative RT-PCR

Total mRNA was extracted from 20 fresh frozen AVM samples (10–300 mg) using QIAzol Lysis Reagent, a RNeasy Lysis Reagent, and RNeasy kit with on-column DNase-digestion (Qiagen, Valencia, CA). cDNA was generated using the iScript cDNA Synthesis kit (Invitrogen, Grand Island, NY). A standard program was used (50°C for 2 min, 95°C for 10 min and (95°C 15 sec, 60°C 1 min) for 40 cycles) for the BioRad CFX96 Real-Time qPCR System. Human-specific primers are listed in Table S1 (Applied Biosystems, Foster City, CA). Primer efficiency and specificity were determined using a pooled sample of brain AVM cDNA and normal human brain tissue. Samples were analyzed in duplicate with threshold cycle (CT) values all within 0.5. CT values were averaged, converted to Δ CT (relative to glyceraldehyde 3-phosphate dehydrogenase (GAPDH)) and to $2^{\Delta\text{CT}}$, which was defined as “Relative expression”.

Tissue culture

HUVECs were purchased from Lonza (Walkersville, MD) and grown according to supplier's instructions in Endothelial Basal Medium-2 (EBM-2) supplemented with Endothelial Growth Medium-2 (EGM-2) SingleQuots. HUVECs were not used beyond passage 10.

Lentiviral-mediated COUP-TFII expression

Lentiviral particles were generated using a vector containing an internal ribosomal entry site (IRES) preceding GFP (pHR-IG) and packaging (p-delta) and envelope plasmids (VSVG). COUP-TFII-IRES-GFP was constructed using cDNA for COUP-TFII (Genbank NM_021005.3; OpenBio-systems, Lafayette, CO). The empty plasmid (IRES-GFP) was used as a control. Lentivirus was produced in HEK293Ts, filtered, concentrated, re-suspended in phosphate buffered saline (PBS), and stored at -80°C . Lentivirus was titered and used at a 1:500. Expression of COUP-TFII was confirmed by western blot analysis using

anti- β -Actin (Sigma-Aldrich, St. Louis, MO, 1:5000) as a loading control and qRT-PCR.

EC proliferation assay

HUVECs stably expressing either COUP-TFII-IRES-GFP or IRES-GFP (“HUVEC-COUP-TFII” and “HUVEC-GFP”, respectively) were cultured at 70,000 cells/mL in EGM-2 for 48 h. Live cells were counted using trypan blue exclusion in triplicate for four separate lentiviral-infected cultures. Data were normalized to HUVEC-GFP cell growth.

EC tube formation assay

EC tube formation assays were established as previously described in triplicate for three separate lentiviral-infected cultures.²⁴ Briefly, low passage HUVECs overexpressed IRES-GFP or COUP-TFII-IRES-GFP 24 h prior to the assay. ECs were grown for 48 h at 1.5×10^5 cells/mL in Geltrex-coated 96 well plates (BD Biosciences, Minneapolis, MN), labeled with Calcein AM and Hoechst 33342 (Invitrogen, Eugene, OR) and imaged with a Zeiss Axio Observer A1 microscope. Images were processed identically with ImageJ (v.1.46r; National Institutes of Health (NIH), USA) for analysis of tube length, diameter, surface area, and number of branches. For surface area, the images were converted to binary with a set scale and analyzed with the Particle Analyzer. For both tube length (the distance between cell clusters) and width (the linear diameter of the tube), an identical grid was applied to fluorescent images and both were determined using the Region Of Interest (ROI) Manager and measure functions. Tube length was determined only for tubes that had clear start and end points. Tube diameter was measured perpendicular from the length for tubes that crossed the counting grid. Branches were defined as the number of tubes radiating from a cell cluster. Hoechst nuclear staining was used to determine the presence of cells.

To ensure normal angiogenic responses following lentiviral infection, EC response was evaluated in four conditions consisting of EGM-2, EGM-2 containing DL-sulforaphane (Sigma-Aldrich, St. Louis, MO), EBM-2 with hrbFGF (human recombinant fibroblast growth factor, R&D Systems, Minneapolis, MN), and EBM-2 alone.

Statistical analyses

All analyses were carried out using SigmaPlot v 12.0. Spearman Rank Order Correlation was used to test the correlation of gene expression with clinical observations. The Mann–Whitney Rank Sum Test was used to determine statistical significance for in vitro cell proliferation assays.

Results

Patient demographics and clinical history

Patients were treated with surgery alone (S), embolization and surgery (ES), or embolization, stereotactic radiosurgery (CyberKnife), and surgery (ERS) (Table 1). AVMs were evaluated for deep versus superficial and single versus multiple venous drainage, eloquence, edema, gliosis, acute hemorrhage, and Spetzler-Martin (SM) grade. A total of 40 unique AVMs were studied, of which 29 were examined by immunohistochemistry (IHC), 20 by qRT-PCR, and nine by both.

AVMs express COUP-TFII and other proteins associated with lymphatic EC identity

We examined paraffin-embedded AVMs for expression of COUP-TFII, PECAM, PROX1, LYVE1, and D2-40 (Podoplanin). PECAM is a pan-EC marker, while PROX1 is

essential for lymphatic EC development and interacts directly with COUP-TFII to determine venous versus lymphatic EC fate.^{17,25} LYVE1 is expressed in lymphatic ECs but is also expressed in developing blood vessels and macrophages.²⁶ D2-40 (Podoplanin) labels lymphatic ECs and is expressed in various tumors, including glioblastomas.²⁷

COUP-TFII was heterogeneously expressed in all 29 AVM samples, with regions of intense and weak immunoreactivity. COUP-TFII protein was highly expressed in the ECs of both large and small vessels, as shown for representative AVMs in Figure 1B, G, and L. In contrast, normal brain vasculature expressed low levels of COUP-TFII (Fig. 1Q). Interneurons also express COUP-TFII and this is likely the identity of the small, positive cells in the normal brain tissue.²⁸ Abundant and variable expression of PROX1 and LYVE1 was evident in the ECs of all AVMs, as illustrated in the representative AVMs in Figure 1C, H, and M for PROX1 and Figure 1D, I, and N for LYVE1. D2-40 (Podoplanin) expression was defined to discrete

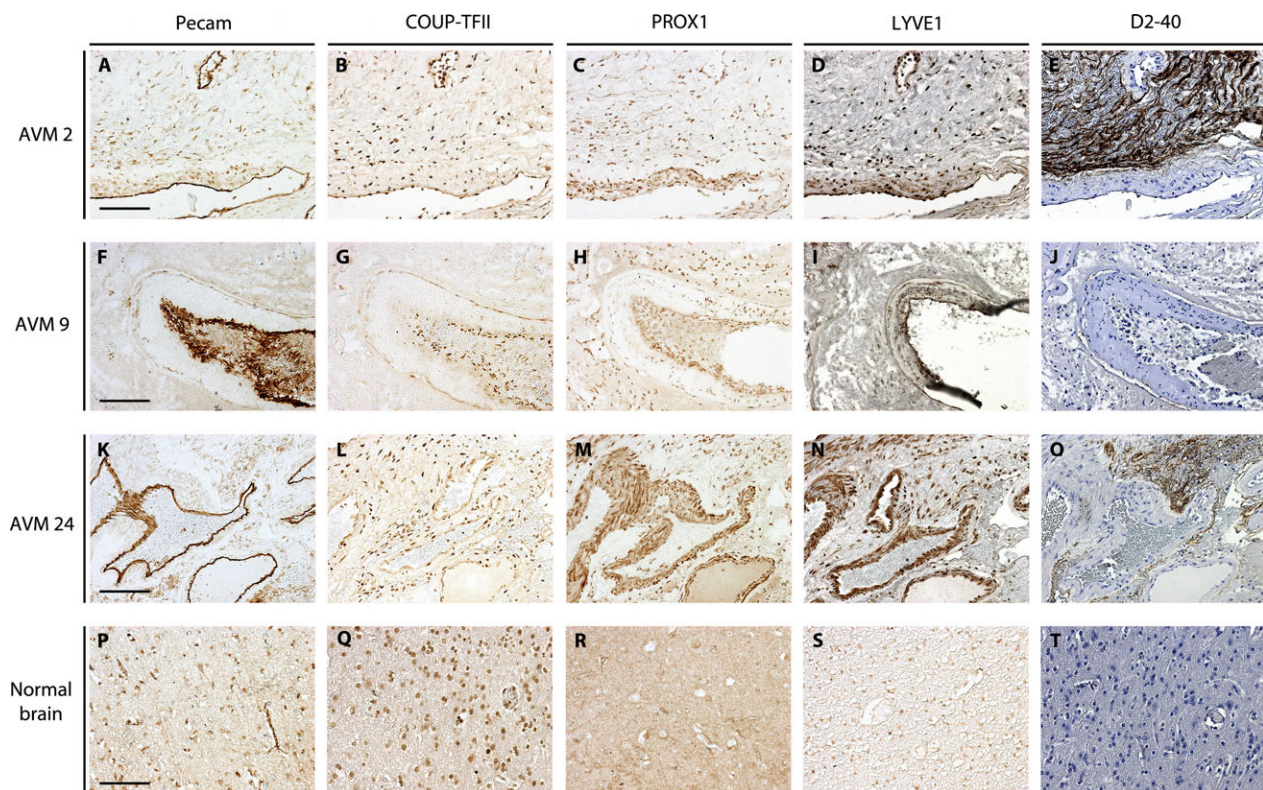


Figure 1. Human brain AVMs express COUP-TFII and other lymphatic-associated proteins in PECAM-positive cells. Representative IHC images of three human brain AVMs illustrate regions of co-expression of COUP-TFII (B, G, and L), PROX1 (C, H, and M), LYVE1 (D, I, and N), and D2-40 (Podoplanin) (E, J, and O) with PECAM-positive ECs (A, F, and K). PECAM-negative cells in the tissue of the AVM also express COUP-TFII. Normal brain contained numerous PECAM-positive ECs (P) but there was minimal expression of COUP-TFII (Q), PROX1 (R), LYVE1 (S), and D2-40 (Podoplanin) (T). DAB-positive immunoreactivity appears as brown staining in the tissue. Scale bar is 50 μ m. AVMs, arteriovenous malformations; IHC, immunohistochemistry; ECs, endothelial cells.

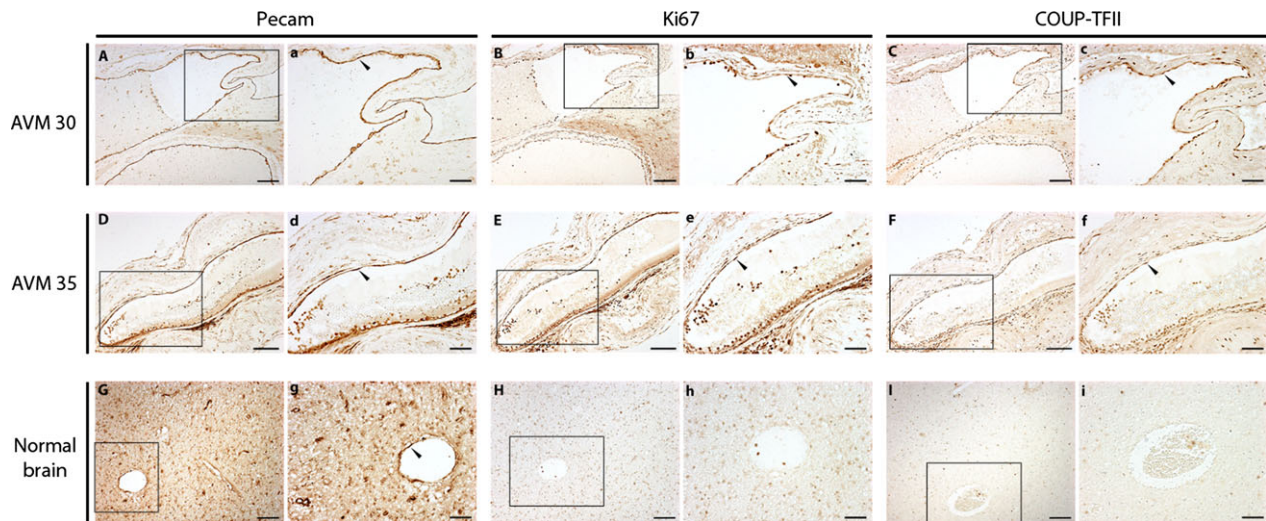


Figure 2. Human brain AVMs contain proliferating ECs. All 29 AVMs contained ECs that were Ki67 positive. As shown in representative images from two AVMs, Ki67-positive cells were present in the same region of the vessels as PECAM- and COUP-TFII-expressing cells (A–F). Normal brain tissue contained numerous PECAM-positive cells (G) but there was minimal expression of both Ki67 (H) and COUP-TFII (I). Higher magnification images of the boxed regions are shown in (a–i). Arrowheads identify regions of co-expression. DAB-positive immunoreactivity appears as brown staining in the tissue. Scale bar is 100 μm for (A–I) and 50 μm for (a–i). AVMs, arteriovenous malformations; ECs, endothelial cells; DAB, 3,3'-diaminobenzidine.

regions of the AVMs (Fig. 1E, J, and O). In contrast, normal human cortex expressed low levels of all of these proteins (Fig. 1Q–T). We confirmed mRNA expression of COUP-TFII, PROX1, and LYVE1 for nine of these AVMs and normal brain using qRT-PCR. Corresponding IHC images and qRT-PCR expression levels of COUP-TFII, PROX1, and LYVE1 for two representative AVMs and normal human cortex are shown in Figure S1.

To determine if brain AVMs were actively proliferating, we also examined expression of Ki67, a cell proliferation marker. There was strong, heterogeneous Ki67 expression in ECs of all 29 AVM samples, as shown for two representative AVMs in Figure 2B(b) and E(e). Ki67 expression corresponded to the region of COUP-TFII expression in PECAM-positive ECs in the AVMs (Fig. 2C(c), and F(f)). In contrast, normal brain contained few Ki67-positive cells (Fig. 2H(h)), despite the presence of many PECAM-positive ECs (Fig. 2G(g)).

AVMs express genes associated with lymphatic specification

To determine if AVMs express other genes associated with lymphatic development, we examined the expression of SOX18, FOXC2, NFATC1, TBX1, and VEGF-C, along with COUP-TFII, PROX1, and LYVE1 by qRT-PCR. SOX18 regulates arteriovenous specification and developmental lymphangiogenesis by regulating expression of PROX1, and is found at low levels in the adult

human brain.^{18,29} Similarly, FOXC2 functions in arterial specification and lymphangiogenesis³⁰ and its transcriptional regulation involves NFATC1, a TF with roles in lymphatic patterning.³¹ TBX1 regulates the expression of VEGFR3 and is essential for lymphatic vessel maturation.³² VEGF-C is a necessary ligand for PROX1-mediated lymphatic development, interacts with SOX18 to regulate lymphangiogenesis,³³ and is the preferred ligand of VEGFR3, a receptor with a role in lymphatic development.³⁴ We also examined the expression of two genes not associated with a lymphatic phenotype: Nestin, a gene that is expressed by neural stem/progenitor cells and has also been observed in human AVMs,^{35,36} and beta-2-microglobulin (B2M), a component of the major histocompatibility complex and associated with peripheral arterial disease.³⁷

The expression of these genes for all 20 AVMs and normal cortex is shown in the heat map in Figure 3A, while the expression of Nestin and B2M is shown in Figure 3B. We defined a “Lymphatic Signature” (LS) as the sum of the expression of the lymphatic-associated genes, including COUP-TFII, SOX18, PROX1, NFATC1, FOXC2, TBX1, LYVE1, and VEGF-C. There was heterogeneity in both the profile and the level of expression of the lymphatic-associated genes across all AVM samples. Of note, PROX1 was highly expressed compared to other genes in the subset of AVMs (13–17, 19) from patients that presented with acute hemorrhage prior to surgery. There was significant correlation between the expressions

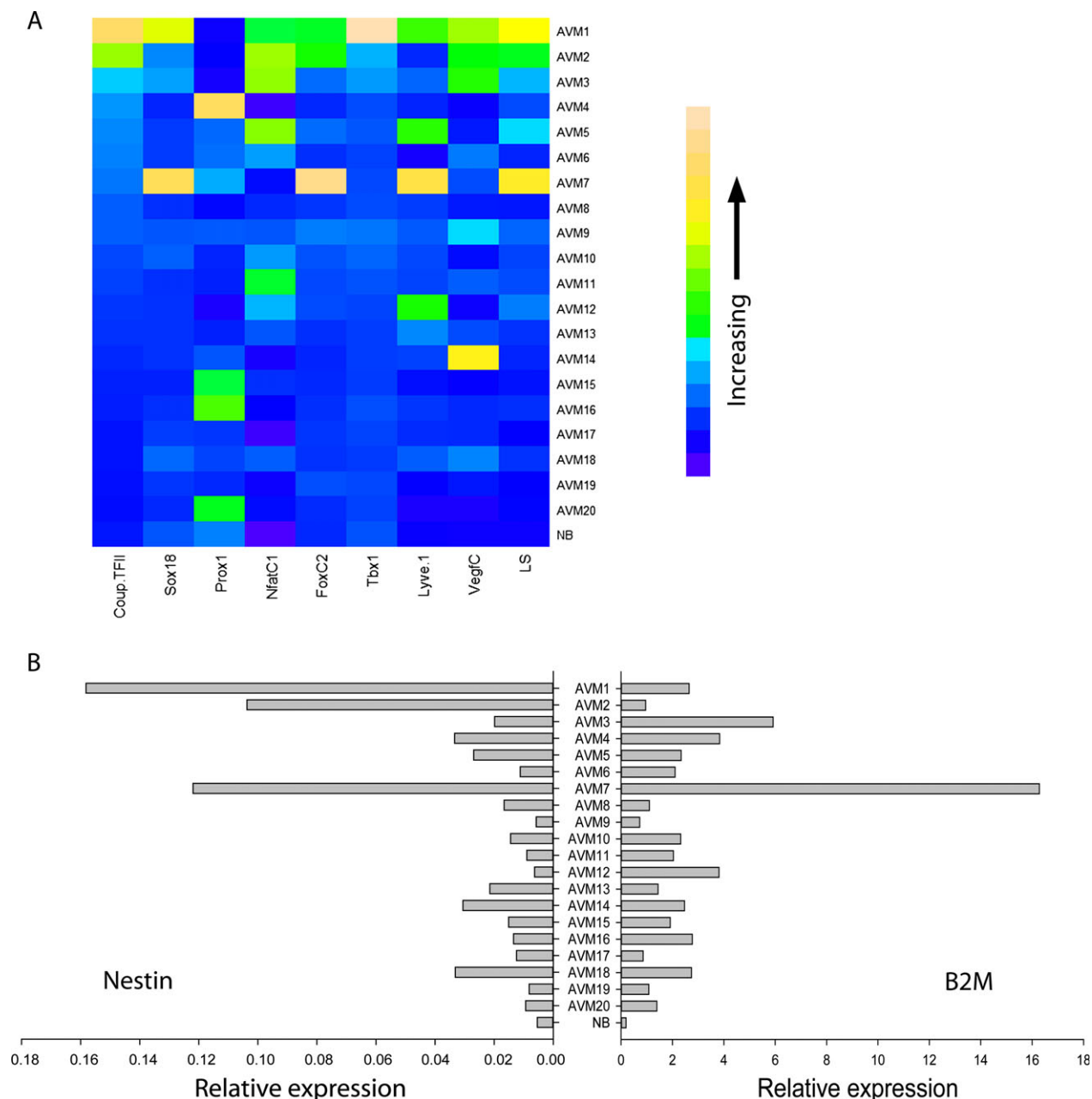


Figure 3. Summary of AVM and normal brain gene expression by qRT-PCR. (A) The heat map represents the relative expression levels of eight lymphatic-associated genes for 20 AVM samples and normal human brain (NB). LS = sum of expression of lymphatic-associated genes (COUP-TFII, SOX18, PROX1, NFATC1, FOXC2, TBX1, LYVE1, and VEGF-C). (B) Expression levels of Nestin (left panel) and B2M (right panel) for the same 20 AVM samples and normal human brain (NB). Samples were analyzed in duplicate with threshold cycle (CT) values all within 0.5. AVM, arteriovenous malformation; VEGF, vascular endothelial growth factor.

of lymphatic-associated genes as outlined in Table 2. COUP-TFII expression positively correlated with SOX18, NFATC1, FOXC2, and TBX1; SOX18 expression positively correlated with NFATC1, FOXC2, LYVE1, and VEGF-C; NFATC1 expression positively correlated with FOXC2 and TBX1; and FOXC2 expression positively correlated with TBX1 and LYVE1. The expression of PROX1

correlated negatively with SOX18, NFATC1, and FOXC2. The LS set of genes correlated significantly with COUP-TFII, SOX18, NFATC1, FOXC2, TBX1, and LYVE1. While this does not indicate a direct interaction between these genes, there was very little correlation observed between these genes and the expression of Nestin and B2M. Significant correlation existed only between Nestin

Table 2. Summary of association of expression levels of lymphatic and nonlymphatic genes with Spetzler-Martin (SM) grade, clinically observed edema and acute hemorrhage in AVMs using Spearman Rank Order Correlation.

Variable	SM	Edema	AH	COUP-TFII	Sox18	PROX1	NfatC1	FoxC2	TBX1	LYVE1	VEGF-C	LS	Nestin	B2M
SM	-													
Edema		-												
CC	0.20													
P val	0.47													
n	15													
AH			-											
CC	-0.01													
P val	0.38													
n	20													
COUP-TFII		0.13	-0.57	-										
CC	0.39	0.65	9e-3**											
P val	20	15	20											
n														
SOX18					-									
CC	0.02	0.44	-0.47	0.45										
P val	0.94	0.10	0.04*	0.05*										
n	20	15	20	20										
PROX1						-								
CC	-0.01	-0.25	0.21	-0.30										
P val	0.98	0.35	0.37	0.20	0.05*									
n	20	15	20	20	20									
NFATC1							-							
CC	0.33	0.47	-0.39	0.55	0.46	-0.60								
P val	0.15	0.07	0.09	0.01**	0.04*	6e-3**								
n	20	15	20	20	20	20								
FOXC2								-						
CC	-0.005	0.44	-0.51	0.50	0.77	-0.48	0.55							
P val	0.98	0.10	0.02*	0.02*	2e-7**	0.03*	0.01**							
n	20	15	20	20	20	20	20							
TBX1									-					
CC	-0.09	-0.06	-0.57	0.68	0.42	-0.36	0.45	0.72						
P val	0.70	0.82	9e-3**	8e-4**	0.06	0.15	0.05*	3e-4**						
n	20	15	20	20	20	20	20	20						
LYVE1										-				
CC	0.32	0.50	-0.37	0.37	0.55	-0.42	0.43	0.57	0.28					
P val	0.17	0.05*	0.11	0.10	0.01**	0.07	0.06	9e-4**	0.23					
n	20	15	20	20	20	20	20	20	20					
VEGF-C											-			
CC	0.004	0.13	-0.19	0.38	0.58	-0.34	0.36	0.29	0.27	0.33				

(Continued)

Table 2. Continued.

Variable	SM	Edema	AH	COUP-TFII	Sox18	PROX1	NfatC1	FoxC2	TBX1	LYVE1	VEGF-C	LS	Nestin	B2M
P val	0.98	0.65	0.41	0.09	8e-3**	0.15	0.12	0.21	0.25	0.15				
n	20	15	20	20	20	20	20	20	20	20				
LS														
CC	0.15	0.57	-0.57	0.76	0.58	-0.29	0.60	0.68	0.61	0.73	0.37			
P val	0.52	0.03*	9e-3**	2e-7**	8e-3**	0.21	5e-3**	8e-4**	4e-3**	1e-4**	0.12			
n	20	15	20	20	20	20	20	20	20	20	20			
Nestin														
CC	-0.05	0.35	-0.13	0.50	0.35	0.005	0.10	0.14	0.14	0.36	0.37	0.50		
P val	0.82	0.20	0.58	0.03*	0.13	0.98	0.66	0.54	0.56	0.12	0.10	0.03*		
n	20	15	20	20	20	20	20	20	20	20	20	20		
B2M														
CC	0.31	0.44	-0.29	0.28	0.14	0.08	0.09	-0.006	0.02	0.47	0.02	0.50	0.43	
P val	0.18	0.10	0.21	0.23	0.55	0.72	0.71	0.98	0.93	0.04*	0.92	0.03*	0.06	
n	20	15	20	20	20	20	20	20	20	20	20	20	20	

Significant correlations are shown in bold. SM, Spetzler-Martin; AH, acute hemorrhage; VEGF, vascular endothelial growth factor; CC, correlation coefficient; P val = P value * \leq 0.05, ** \leq 0.01; n, number of samples; LS, sum of expression of lymphatic-associated genes (COUP-TFII, SOX18, PROX1, NFATC1, FOXC2, TBX1, LYVE1, and VEGF-C).

and COUP-TFII, and between B2M and LYVE1; both Nestin and B2M correlated with the LS gene set.

Edema and acute hemorrhage correlate with lymphatic-associated genes

We determined if there was any association between gene expression and clinical aspects of AVMs. There was a significant positive correlation with preoperative edema and the expression of LYVE1 ($P = 0.05$) and the LS ($P = 0.03$), as shown in Table 2. Acute hemorrhage was significantly negatively correlated with COUP-TFII ($P = 0.009$), SOX18 ($P = 0.04$), FOXC2 ($P = 0.02$), TBX1 ($P = 0.009$), and LS ($P = 0.009$). AVMs from patients with acute hemorrhage prior to surgery are labeled AVM13-17 and AVM19 in the heat map in Figure 3A, illustrating the unique expression profiles of these samples. There were no significant correlations between gene expression and SM Grade, gliosis, venous drainage, eloquence, and age with the exception of a single correlation between eloquence and B2M ($P = 0.004$).

Heterogeneous expression of key signaling pathway genes

To gain insight into potential signaling mechanisms, we further examined the expression of selected genes involved in arterial and venous specification pathways, including HH, Notch, VEGF, and Wnt (as reviewed in³⁸) in a subset of 14 AVMs and normal brain by qRT-PCR. We analyzed the expression of IHH, SHH and DHH (Fig. 4A), PTCH1 (a HH receptor) and GLI1 (mediates HH signaling) (Fig. 4B), HEY2 (downstream effector of Notch), and VEGFA (ligand for both VEGFR1 and VEGFR2) (Fig. 4C). HH signaling is crucial in vascular development but there is also evidence for a HH response element in the COUP-TFII promoter.³⁹ We also examined the expression of BRG1 and CHD4, two genes that modulate Wnt signaling in angiogenesis⁴⁰ (Fig. 4D). BRG1 has also recently been shown to regulate COUP-TFII expression.⁴¹ Expression of these genes varied across the AVMs compared to normal brain, with strong expression of IHH, DHH, PTCH1, HEY2m VEGFA, and BRG1 in several AVMs. There was nothing clinically remarkable for these particular AVMs.

Increased EC proliferation in vitro with COUP-TFII overexpression

To determine the effect of COUP-TFII on ECs in vitro, we examined the proliferation of HUVEC-COUP-TFII and HUVEC-GFP at 48 h. As is shown in Figure 5, COUP-TFII overexpression significantly increased HUVEC

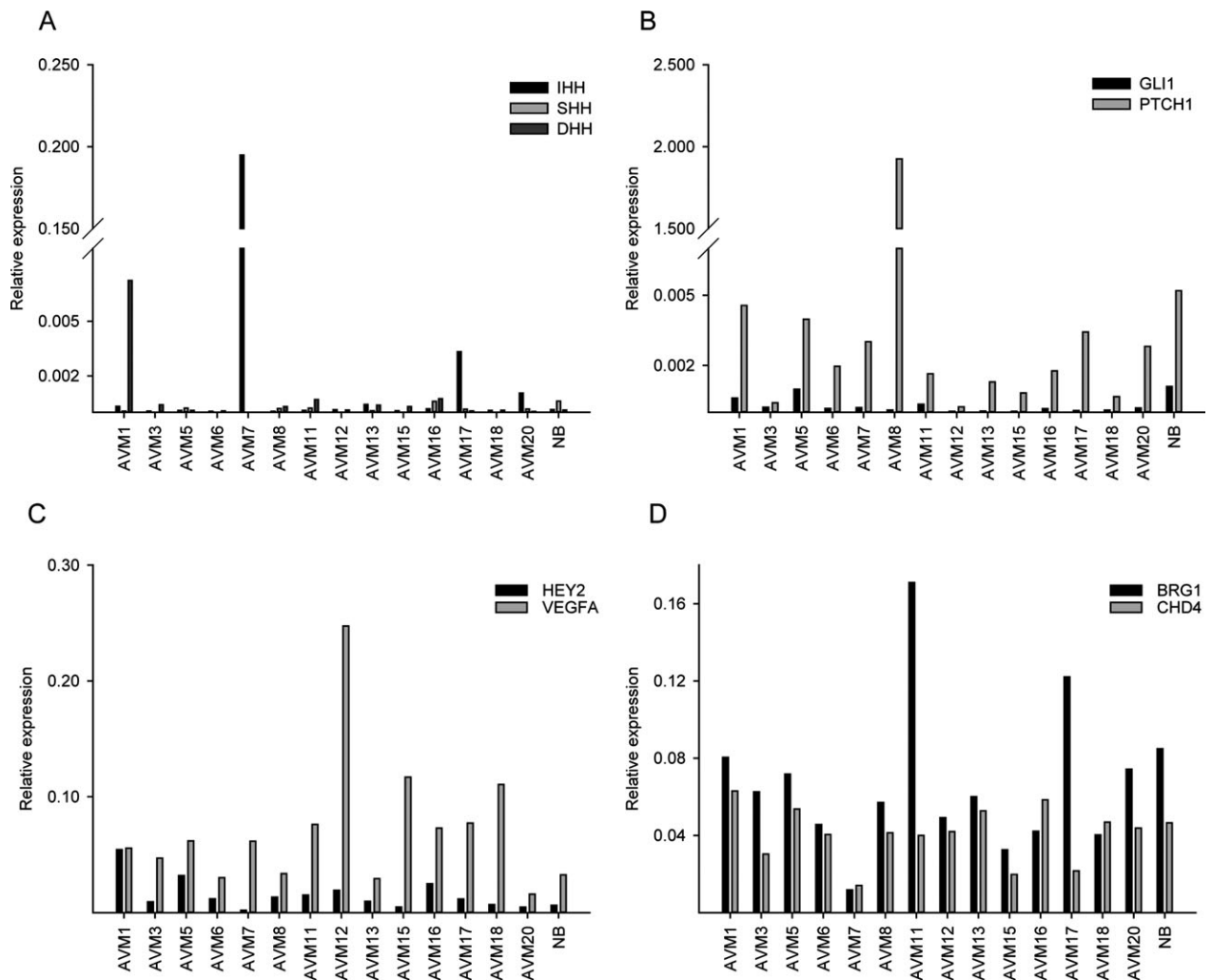


Figure 4. Human brain AVMs heterogeneously expressed selected genes involved in Hedgehog (A, B), Notch (C), VEGF (C), and Wnt (D) pathways. A subset of 14 AVM samples and normal brain (NB) were analyzed by qRT-PCR in duplicate with CT values within 0.5 CT. AVM, arteriovenous malformation; VEGF, vascular endothelial growth factor; CT, threshold cycle.

proliferation ($P \leq 0.001$) relative to control. Overexpression of COUP-TFII mRNA and protein was confirmed by qRT-PCR and western blot (Fig. S2A and B).

COUP-TFII overexpression results in dilated EC tubes

To determine if COUP-TFII had an effect on angiogenesis, we used the *in vitro* EC tube formation assay to examine tube formation at 48 h for HUVEC-GFP and HUVEC-COUP-TFII. HUVECs maintained normal angiogenic responses to EGM-2, EGM-2 with sulforaphane (a broad-based inhibitor of angiogenesis), EBM-2 with FGF and EBM-2 (Fig. S3). Representative images of tube formation for HUVEC-GFP and HUVEC-COUP-TFII visualized with Calcein AM are shown in Figure 6A and B,

respectively. There was no significant difference in tube length (Fig. 6C) but there was a trend toward increased branch points with COUP-TFII overexpression (Fig. 6D). There was a significant increase in tube surface area (Fig. 6E, $P = 0.002$) and tube width (Fig. 6F, $P \leq 0.001$) in HUVEC-COUP-TFII compared to HUVEC-GFP cells. This effect was not due to differences in proliferation, as confirmed by quantitation of RNA extracted from individual wells of HUVEC-COUP-TFII and HUVEC-GFP (data not shown).

Discussion

The mechanisms by which AVMs develop are still largely unknown. There is exquisite control over EC specification and arterial, venous, and lymphatic development, with

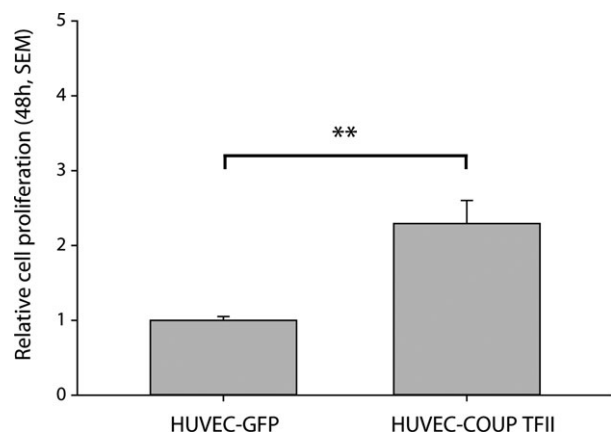


Figure 5. COUP-TFII overexpression results in increased proliferation in HUVECs. Cell proliferation was determined at 48 h for HUVEC-GFP and HUVEC-COUP-TFII ($n = 4$ independent lentiviral-infected HUVEC cultures). Data are presented relative to HUVEC-GFP proliferation. SEM, standard error of the mean; $**P \leq 0.001$. HUVECs, human umbilical endothelial cells.

key roles for Notch, COUP-TFII and PROX; dysregulation of any of these genes, and other genes involved in vascular development and maintenance, results in vascular pathology as demonstrated in both animal models and humans. In rodents, both loss-of- and gain-of-function Notch signaling have been shown to generate vascular malformations,^{42,43} while normalization of Notch signaling leads to malformation regression.¹⁰ Overexpression of COUP-TFII in vivo also resulted in vascular malformations in a conditional, EC-specific mouse model¹⁶ and in vitro overexpression of COUP-TFII alone can downregulate HEY2, a downstream target of Notch signaling.⁴⁴ Finally, EC-specific overexpression of PROX1 results in hemorrhage, edema, anemia, and embryonic lethality at E13.5, possibly due to alterations in tight junction proteins such as ZO-1 and Occludin.⁴⁵ Expression of these proteins in human AVMs has not been fully studied previously, although there is some evidence for activated Notch-1 signaling.^{46,47} AVMs are known to occur via other mechanisms, however. Hereditary hemorrhagic telangiectasia (HHT), a disease with a high incidence of brain AVMs, is frequently associated with gene mutations in ENG (HHT type 1), ACVRL1 (HHT type 2), or SMAD4, all of which ultimately result in disrupted TGF β signaling.⁴⁸ The recent report of the disruption of TGF β signaling via a direct interaction between COUP-TFII and SMAD4 suggests a role for COUP-TFII in modulating TGF β signaling directly.²¹ These diverse molecular pathways provide support that AVMs may form via independent mechanisms despite a seemingly homogeneous disease phenotype. While the varied expression of selected signaling pathway genes shown here does not illustrate a

clear signaling pathway or mechanism, it does suggest that the underlying disease biology of human brain AVMs is complex, and points to potential underlying disease heterogeneity or to changes in AVM biology from patient to patient depending on when the AVM was diagnosed and removed. Future experiments will address these issues.

The work we present here suggests a previously undescribed role for COUP-TFII, PROX1, and other angiogenesis/lymphatic-associated genes in human brain AVMs. We have shown that human brain AVMs express COUP-TFII and other genes known to regulate key aspects of angiogenesis and lymphangiogenesis. The expression of these genes significantly correlated with each other, and a subset significantly correlated with the presence of preoperative edema and acute hemorrhage. We have also shown that AVMs contain Ki67-positive proliferating cells and that overexpression of COUP-TFII in vitro resulted in both increased EC proliferation and dilated tubes in an EC tube formation assay. The trend toward comparatively higher levels of PROX1 expression in the AVMs from patients presenting with acute hemorrhage is also intriguing, given that PROX1 alone is capable of reprogramming vascular ECs to the lymphatic fate in vivo,⁴⁵ and is normally involved in the development of the lymphatic system.³⁴ COUP-TFII has previously been shown to initiate PROX1 transcription, and although not necessary for the maintenance of expression, may potentially be initiating PROX1 expression in AVMs.¹⁹ Increased levels of PROX1 may also simply be a consequence of acute hemorrhage and future work will be required to address the question of PROX1 expression and compromised vascular integrity, edema, and hemorrhage.

It remains unclear whether COUP-TFII overexpression is an initiating event in AVM formation, or if normal COUP-TFII expression is dysregulated during development or activated post development. A challenge to studying human tissue is that it is not possible to examine the temporal or dynamic expression that might be occurring throughout the initiation, development, and maintenance of the AVM. The question also remains by what mechanism COUP-TFII, a transcription factor largely absent from normal mature cerebrovasculature, is being expressed in brain AVMs. The transcriptional regulation of COUP-TFII is not well understood, including how cerebrovascular ECs are restricted in their ability to acquire a lymphatic fate during development. Interestingly, a HH response element has been identified in the COUP-TFII promoter region,³⁹ and more recent work has shown the chromatin-remodeling enzyme BRG1 functions during normal development to promote the expression of COUP-TFII in vascular endothelium.⁴¹ It is also critical to assess is the contribution of flow-induced

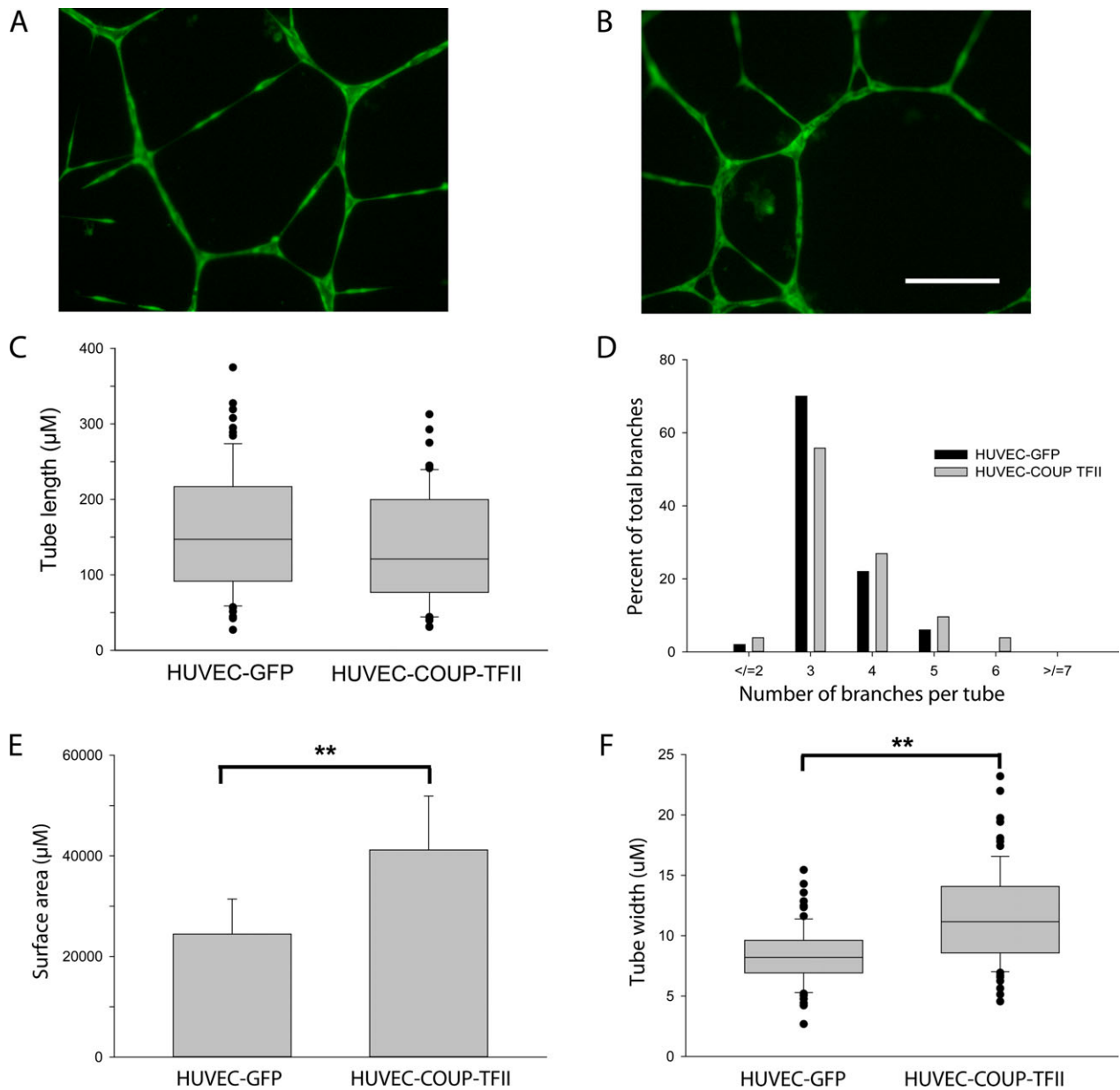


Figure 6. COUP-TFII overexpression results in dilated EC tubes. Representative images of tube formation of HUVEC-GFP (A) and of HUVEC-COUP-TFII (B) after 48 h. Tube length was not significantly different in HUVEC-COUP-TFII (C), while there was a trend toward more branching in HUVEC-COUP-TFII (D). Both the surface area (E) and the tube width (F) were significantly increased in HUVEC-COUP-TFII cultures. $N = 3$ independent lentiviral-infected cultures. Scale bar $200 \mu\text{m}$; $**P \leq 0.002$. EC, endothelial cell; HUVEC, human umbilical endothelial cell.

mechanical stress. Studies in a zebrafish model of HHT demonstrate the crucial role of hemodynamic forces in AVM formation and gene expression¹²; however, the contribution of aberrant blood flow to gene expression in human brain AVMs is currently unknown. AVMs present a lower resistance vascular bed owing to the lack of a capillary network, and experience nonuniform wall shear stress ranging from 40 to 72 dynes per cm^2 , well beyond the normal range.¹ Development of additional in vivo

and in vitro models of AVMs may address these questions and further elucidate disease mechanisms.

The expression of lymphatic-associated genes in brain AVMs is interesting, given that the normal brain does not have the classic lymphatic vascular system that exists in the rest of the body. There is evidence for additional cerebrovascular irregularities in AVMs including the presence of Weibel-Palade bodies which are largely absent in normal brain ECs, a compromised blood-brain barrier, as well as

reduced mural cell coverage.^{49,50} As the molecular events controlling the normal specification, development, and maintenance of the vascular and lymphatic systems are elucidated, so too will those pathological processes involved in cerebrovascular malformations and diseases, including AVMs and brain aneurysms. The work presented here identifies additional potential contributors to AVM disease biology and has highlighted further avenues for research. Clinically, one of the most significant challenges in treating patients with AVMs is the evaluation of hemorrhage risk, upon which hinges the choice of appropriate treatment plan. To gauge the risks of surgical intervention, brain AVMs are commonly classified according to the SM grade; no such criterion is yet available to gauge hemorrhage risk, although there is some preliminary association of AVM size, protein expression, and single nucleotide polymorphisms (SNPs) with higher risks of hemorrhage.^{1,8} This work may have important future implications for improving clinicians' abilities to predict AVM hemorrhage risk. Additional studies of AVM patients and state-of-the-art imaging techniques may address this question and provide additional clinical correlates to these basic research findings.

Acknowledgments

We thank the Stanford patients and their families, the Neurosurgery Clinical Research team, Garrison Fathman and Nate Manley for the lentiviral constructs, and the Steinberg and Chang laboratories for helpful discussions and critical reading of the manuscript. We also thank the Stanford Neuropathology and Pathology Departments for assistance in sectioning the paraffin-embedded slides and for the D2-40 staining.

Conflict of Interest

None declared.

References

- Moftakhar P, Hauptman JS, Malkasian D, Martin NA. Cerebral arteriovenous malformations. Part 2: physiology. *Neurosurg Focus* 2009;26:E11.
- Sure U, Butz N, Schlegel J, et al. Endothelial proliferation, neoangiogenesis, and potential de novo generation of cerebrovascular malformations. *J Neurosurg* 2001;94:972–977.
- Hashimoto T, Mesa-Tejada R, Quick CM, et al. Evidence of increased endothelial cell turnover in brain arteriovenous malformations. *Neurosurgery* 2001;49:124–131; discussion 131–122.
- Jabbour MN, Elder JB, Samuelson CG, et al. Aberrant angiogenic characteristics of human brain arteriovenous malformation endothelial cells. *Neurosurgery* 2009;64:139–146; discussion 146–138.
- Wautier M-P, Boval B, Chappey O, et al. Cultured endothelial cells from human arteriovenous malformations have defective growth regulation. *Blood* 1999;94:2020–2028.
- Stapleton CJ, Armstrong DL, Zidovetzki R, et al. Thrombospondin-1 modulates the angiogenic phenotype of human cerebral arteriovenous malformation endothelial cells. *Neurosurgery* 2011;68:1342–1353.
- Laakso A, Hernesniemi J. Arteriovenous malformations: epidemiology and clinical presentation. *Neurosurg Clin N Am* 2012;23:1–6.
- Kim H, Marchuk DA, Pawlikowska L, et al. Genetic considerations relevant to intracranial hemorrhage and brain arteriovenous malformations. *Acta Neurochir Suppl* 2008;105:199–206.
- Moftakhar P, Hauptman JS, Malkasian D, Martin NA. Cerebral arteriovenous malformations. Part 1: cellular and molecular biology. *Neurosurg Focus* 2009;26:E10.
- Murphy PA, Kim TN, Lu G, et al. Notch4 normalization reduces blood vessel size in arteriovenous malformations. *Sci Transl Med* 2012;4:117ra118.
- Tu J, Karunanayaka A, Windsor A, Stoodley MA. Comparison of an animal model of arteriovenous malformation with human arteriovenous malformation. *J Clin Neurosci* 2010;17:96–102.
- Corti P, Young S, Chen C-Y, et al. Interaction between alk1 and blood flow in the development of arteriovenous malformations. *Development* 2011;138:1573–1582.
- Park SO, Wankhede M, Lee YJ, et al. Real-time imaging of de novo arteriovenous malformation in a mouse model of hereditary hemorrhagic telangiectasia. *J Clin Invest* 2009;119:3487–3496.
- Lin F-J, Qin J, Tang K, et al. Coup d'Etat: an orphan takes control. *Endocr Rev* 2011;32:404–421.
- Chen X, Qin J, Cheng C-M, et al. COUP-TFII Is a major regulator of cell cycle and notch signaling pathways. *Mol Endocrinol* 2012;26:1268–1277.
- You L-R, Lin F-J, Lee CT, et al. Suppression of Notch signalling by the COUP-TFII transcription factor regulates vein identity. *Nature* 2005;435:98–104.
- Aranguren XL, Beerens M, Coppiello G, et al. COUP-TFII orchestrates venous and lymphatic endothelial identity by homo- or heterodimerisation with PROX1. *J Cell Sci* 2013;126:1164–1174.
- Francois M, Caprini A, Hosking B, et al. Sox18 induces development of the lymphatic vasculature in mice. *Nature* 2008;456:643–647.
- Srinivasan RS, Geng X, Yang Y, et al. The nuclear hormone receptor Coup-TFII is required for the initiation and early maintenance of Prox1 expression in lymphatic endothelial cells. *Genes Dev* 2010;24:696–707.

20. Pereira FA, Qiu Y, Zhou G, et al. The orphan nuclear receptor COUP-TFII is required for angiogenesis and heart development. *Genes Dev* 1999;13:1037–1049.
21. Qin J, Wu SP, Creighton CJ, et al. COUP-TFII inhibits TGF-beta-induced growth barrier to promote prostate tumorigenesis. *Nature* 2013;493:236–240.
22. Qin J, Chen X, Xie X, et al. COUP-TFII regulates tumor growth and metastasis by modulating tumor angiogenesis. *Proc Natl Acad Sci USA* 2010;107:3687–3692.
23. Qin J, Chen X, Yu-Lee LY, et al. Nuclear receptor COUP-TFII controls pancreatic islet tumor angiogenesis by regulating vascular endothelial growth factor/vascular endothelial growth factor receptor-2 signaling. *Cancer Res* 2010;70:8812–8821.
24. Arnaoutova I, Kleinman HK. In vitro angiogenesis: endothelial cell tube formation on gelled basement membrane extract. *Nat Protoc* 2010;5:628–635.
25. Wigle JT, Oliver G. Prox1 function is required for the development of the murine lymphatic system. *Cell* 1999;98:769–778.
26. Gordon EJ, Gale NW, Harvey NL. Expression of the hyaluronan receptor LYVE-1 is not restricted to the lymphatic vasculature; LYVE-1 is also expressed on embryonic blood vessels. *Dev Dyn* 2008;237:1901–1909.
27. Nakamura Y, Kanemura Y, Yamada T, et al. D2-40 antibody immunoreactivity in developing human brain, brain tumors and cultured neural cells. *Mod Pathol* 2006;19:974–985.
28. Reinchisi G, Ijichi K, Glidden N, et al. COUP-TFII expressing interneurons in human fetal forebrain. *Cereb Cortex* 2012;22:2820–2830.
29. Pennisi DJ, James KM, Hosking B, et al. Structure, mapping, and expression of human SOX18. *Mamm Genome* 2000;11:1147–1149.
30. Seo S, Fujita H, Nakano A, et al. The forkhead transcription factors, Foxc1 and Foxc2, are required for arterial specification and lymphatic sprouting during vascular development. *Dev Biol* 2006;294:458–470.
31. Normén C, Ivanov KI, Cheng J, et al. FOXC2 controls formation and maturation of lymphatic collecting vessels through cooperation with NFATc1. *J Cell Biol* 2009;185:439–457.
32. Chen L, Mupo A, Huynh T, et al. Tbx1 regulates Vegfr3 and is required for lymphatic vessel development. *J Cell Biol* 2010;189:417–424.
33. Cermenati S, Moleri S, Neyt C, et al. Sox18 genetically interacts with VegfC to regulate lymphangiogenesis in zebrafish. *Arterioscler Thromb Vasc Biol* 2013;33:1238–1247.
34. Wigle JT, Harvey N, Detmar M, et al. An essential role for Prox1 in the induction of the lymphatic endothelial cell phenotype. *EMBO J* 2002;21:1505–1513.
35. Shimizu T, Sugawara K, Tosaka M, et al. Nestin expression in vascular malformations: a novel marker for proliferative endothelium. *Neurol Med Chir (Tokyo)* 2006;46:111–117.
36. Ha Y, Kim TS, Yoon DH, et al. Reinduced expression of developmental proteins (nestin, small heat shock protein) in and around cerebral arteriovenous malformations. *Clin Neuropathol* 2003;22:252–261.
37. Wilson AM, Kimura E, Harada RK, et al. β 2-microglobulin as a biomarker in peripheral arterial disease: proteomic profiling and clinical studies. *Circulation* 2007;116:1396–1403.
38. Corada M, Morini MF, Dejana E. Signaling pathways in the specification of arteries and veins. *Arterioscler Thromb Vasc Biol* 2014;34:2372–2377.
39. Krishnan V, Elberg G, Tsai MJ, Tsai SY. Identification of a novel sonic hedgehog response element in the chicken ovalbumin upstream promoter-transcription factor II promoter. *Mol Endocrinol* 1997;11:1458–1466.
40. Curtis CD, Griffin CT. The chromatin-remodeling enzymes BRG1 and CHD4 antagonistically regulate vascular Wnt signaling. *Mol Cell Biol* 2012;32:1312–1320.
41. Davis RB, Curtis CD, Griffin CT. BRG1 promotes COUP-TFII expression and venous specification during embryonic vascular development. *Development* 2013;140:1272–1281.
42. Murphy PA, Lam MT, Wu X, et al. Endothelial Notch4 signaling induces hallmarks of brain arteriovenous malformations in mice. *Proc Natl Acad Sci USA* 2008;105:10901–10906.
43. Krebs LT, Starling C, Chervonsky AV, Gridley T. Notch1 activation in mice causes arteriovenous malformations phenocopied by ephrinB2 and EphB4 mutants. *Genesis* 2010;48:146–150.
44. Korten S, Brunssen C, Poitz DM, et al. Impact of Hey2 and COUP-TFII on genes involved in arteriovenous differentiation in primary human arterial and venous endothelial cells. *Basic Res Cardiol* 2013;108:362.
45. Kim H, Nguyen V, Petrova T, et al. Embryonic vascular endothelial cells are malleable to reprogramming via Prox1 to a lymphatic gene signature. *BMC Dev Biol* 2010;10:72.
46. Murphy PA, Lu G, Shiah S, et al. Endothelial Notch signaling is upregulated in human brain arteriovenous malformations and a mouse model of the disease. *Lab Invest* 2009;89:971–982.
47. ZhuGe Q, Zhong M, Zheng W, et al. Notch-1 signalling is activated in brain arteriovenous malformations in humans. *Brain* 2009;132:3231–3241.
48. McDonald J, Bayrak-Toydemir P, Pyeritz RE. Hereditary hemorrhagic telangiectasia: an overview of diagnosis, management, and pathogenesis. *Genet Med* 2011;13:607–616.
49. Chen W, Guo Y, Walker EJ, et al. Reduced mural cell coverage and impaired vessel integrity after angiogenic

stimulation in the Alk1-deficient brain. *Arterioscler Thromb Vasc Biol* 2013;33:305–310.

50. Tu J, Stoodley MA, Morgan MK, Storer KP. Ultrastructure of perinidal capillaries in cerebral arteriovenous malformations. *Neurosurgery* 2006;58:961–970; discussion 961–970.

Supporting Information

Additional Supporting Information may be found in the online version of this article:

Figure S1. A comparison of protein and mRNA expression of COUP-TFII, PROX1, and LYVE1 in human AVMs and normal brain. As shown for two representative AVM samples and normal brain, protein expression by IHC (A,A–I) reasonably corresponded to the expression of these proteins by qRT-PCR (B). DAB immunoreactivity appears as brown staining. Samples were analyzed in duplicate with threshold cycle (CT) values all within 0.5. Scale bar is 100 μ m.

Figure S2. Lentiviral-mediated overexpression of IRES-GFP and COUP-TFII-IRES-GFP in HUVECs. Both COUP-TFII mRNA (A) and protein (B) were abundantly expressed in HUVECS following lentiviral-mediated overexpression. GAPDH was the reference gene for qRT-PCR while β -actin was used as loading control for western blot.

Figure S3. Lentiviral-infected HUVECs maintain a normal response in the endothelial tube formation assay. Representative images of HUVEC-GFP and HUVEC-COUP-TFII tube formation using Calcein AM in the presence of fully supportive medium (EGM-2), no tube formation in fully supportive medium containing the angiogenesis inhibitor sulforaphane (EGM-2+ Inhibitor), and reduced tube formation with minimally supportive medium (EBM-2) or in the presence of FGF alone (EBM-2+ FGF). Scale bar is 100 μ m.

Table S1. List of FAMTM qRT-PCR primer sets against human genes (Applied Biosystems, Foster City, CA).